

IAC-04-S.2.b.08

ANALYSIS OF A SOLAR SAIL MERCURY SAMPLE RETURN MISSION

Gareth W. Hughes*, Malcolm Macdonald*, Colin R. McInnes†

*Research Assistant, Dept. of Aerospace Engineering, University of Glasgow, Glasgow, UK

†Professor, Department of Mechanical Engineering, University of Strathclyde, Glasgow, UK
ghughes@aero.gla.ac.uk, m.macdonald@aero.gla.ac.uk, colin.mcinnnes@strath.ac.uk

Alessandro Atzei, Peter Falkner

ESA/ESTEC, Science Payloads and Advanced Concepts Office, Noordwijk, The Netherlands
aatzei@rssd.esa.int, Peter.Falkner@esa.intABSTRACT

A conventional Mercury sample return mission requires significant launch mass, due to the large Δv required for the outbound and return trips, and the large mass of a planetary lander and ascent vehicle. Solar sailing can be used to reduce lander mass allocation by delivering the lander to a low, thermally safe orbit close to the terminator. In addition, the ascending node of the solar sail parking orbit plane can be artificially forced to avoid out-of-plane manoeuvres during ascent from the planetary surface. Propellant mass is not an issue for solar sails so a sample can be returned relatively easily, without resorting to lengthy, multiple gravity assists. A 275 m solar sail with an assembly loading of 5.9 g m^{-2} is used to deliver a lander, cruise stage and science payload to a forced Sun-synchronous orbit at Mercury in 2.85 years. The lander acquires samples, and conducts limited surface exploration. An ascent vehicle delivers a small cold gas rendezvous vehicle containing the samples for transfer to the solar sail. The solar sail then spirals back to Earth in 1 year. The total mission launch mass is 2353 kg, on an H2A202-4S class launch vehicle ($C_3=0$), with a ROM mission cost of 850 M€. Nominal launch is in April 2014 with sample return to Earth 4.4 years later. Solar sailing reduces launch mass by 60% and trip time by 40%, relative to conventional mission concepts.

INTRODUCTIONMercury Science

Of the terrestrial planets, Mercury is the one of which we know the least, its location deep within the solar gravity well ensuring that spacecraft have been sent there infrequently. Mercury's unusual 3:2 spin-orbit resonance meant that the same side was imaged in each of the Mariner 10 flybys. Surface coverage is incomplete and the planet must be comprehensively mapped by an orbiter mission such as BepiColombo or Messenger, before a sample return mission can proceed and a landing site selected. There is no significant water or atmosphere, so that daytime temperatures can soar to 700 K, and plummet to 100 K at night, due to the slow spin period. The lack of CO_2 or H_2O in the atmosphere suggests that Mercury is either intrinsically volatile deficient, or is not out-gassing at a rate

comparable to that of the Earth, and so is less geologically active.¹ Aside from the Earth, Mercury is the only terrestrial planet which is known to have an intrinsic, weak, magnetic field. This is produced either by an Earth-like magnetohydrodynamic dynamo in the core, or a remnant magnetic field in the rock, which could be evident in any surface samples returned. The high average density of 5.43 g m^{-3} could be due to the presence of Iron within the interior, perhaps generated by this Earth-like magnetohydrodynamic dynamo, consistent with electrical currents flowing in a molten core. Tectonically, unique compressive thrust faults called lobate scarps occur on a global scale, implying global compressive stresses in Mercury's distant past. Large impact basins on Mercury can also contain volcanic deposits, which suggests that there has been volcanic activity after the impact. Little is known about the surface geology, composition, and chemistry, therefore sample

return would be of significant benefit. Radar reflection measurements appear to show volatile compounds, possibly water ice, at both poles, deep within the shadows of craters, but observations from Earth are difficult due to the proximity of Mercury to the Sun. The lack of any appreciable atmosphere means that very cold regions exist in polar craters, allowing radar-bright materials to remain.

Science Objectives

It is important to ascertain the surface age of Mercury to understand its geologic history. Accurate rock dating of Mercury surface samples is only possible on Earth. Due to the tenuous atmosphere, the entire descent must be via chemical propulsion. A high-latitude landing site is selected due to thermal constraints, and prior imaging of this site from the orbiter at a resolution of better than 1 metre per pixel is necessary. Even at high latitudes, landing in direct sunlight, or indeed in permanent shadow would be undesirable. A landing site within a suitable crater, in partial shade, but with some light reflected from the crater walls is preferable, with a sample drilled from a rock outcrop within the crater.² However, recent craters may be contaminated with material from their impactor, and should be avoided. Guided descent is employed for all but the last few metres of the descent, since the thruster plume would scorch the landing site, contaminating the surface regolith to be sampled. The stroke of the landing legs is used to absorb the remaining kinetic energy of surface impact.

Baseline science objectives for a Mercury sample return mission are therefore, to acquire a surface sample through a precision landing at a carefully selected high latitude landing site in partial shadow, within a suitably aged crater, with high resolution imaging for documentation during terminal descent. Sample pre-selection and pre-analysis will be conducted in-situ during landing site characterisation using a robotic arm and small mobility device (20 m range).¹ The primary science goal is to acquire 350 g of surface regolith. Mercury is not thought to be of direct interest to exobiology in the solar system, so planetary protection measures will be simpler than for Mars missions, more similar to lunar missions.

Solar Sailing

The extremely high Δv required for Mercury sample return can be met relatively easily by solar sails, since propellant mass is not an issue, significantly reducing launch mass. Lengthy multiple gravity assists are not required, and the launch window is always open in principle. Thermally-safe orbit precession at Mercury is possible using the continuous thrust. Solar sail performance is defined by the Characteristic Acceleration, the solar radiation pressure induced acceleration at 1 AU with the sail normal oriented along the Sun-line.³

PAYLOAD MODEL

A full and detailed solar sail payload has been defined and customised,⁴ based loosely on an internal ESA Assessment Study,¹ with some aspects drawn from a NASA/JPL Team X report.² A trade-off of the optimum solar sail parking orbit at Mercury was conducted so as to minimise the Mercury Ascent Vehicle (MAV) Δv requirements. The use of an artificial Sun-Synchronous polar orbit at Mercury close to the planetary terminator,⁵ can be effected to reduce the thermal loads on the orbiter through a constant precession of the line of nodes, enabling a longer orbiter stay time and much lower parking orbit. The characteristic acceleration of the sail in the parking orbit is defined by the parameters of the Sun-Synchronous orbit, and so as the acceleration is increased the Sun-Synchronous orbit can be increasingly circularised. Fig. 1 shows the effect of rendezvous orbit altitude on MAV launch mass. It is seen that ascent direct to the Sun-Synchronous orbit requires much more Δv than ascent to a circular orbit. A circular 100 km orbit was selected to minimise MAV Δv requirements, with the sail used to deliver the lander onto the 100 km orbit, after an initial 44 day science and landing site selection phase on a 100 x 7500 km forced Sun-Synchronous orbit, 10° ahead of the solar terminator. During sample acquisition, until after coplanar MAV launch, the sail rotates the circular 100 km orbit plane to rendezvous with the MAV orbit, before spiralling to escape.

The solar sail payload stack comprises a small cold-gas Sail Rendezvous Vehicle

(SRV), to conduct proximity manoeuvres when transferring the sample from the MAV to the ballistic Earth Return Vehicle (ERV) attached to the Sail Cruise Stage (SCS). The bi-propellant MAV and cold-gas SRV is mounted on the bi-propellant Mercury Descent Vehicle (MDV). The MDV has a large science platform and 0.4 m^2 Gallium Arsenide solar arrays. Fig. 2 shows the lander deployed with its landing legs extended. Tables 1-4 show the mass breakdown of the SRV, MAV, MDV, and SCS, respectively. An analysis of the spacecraft subsystems, shows a total spacecraft mass of 1905 kg, to support acquisition of 350 g of surface samples.

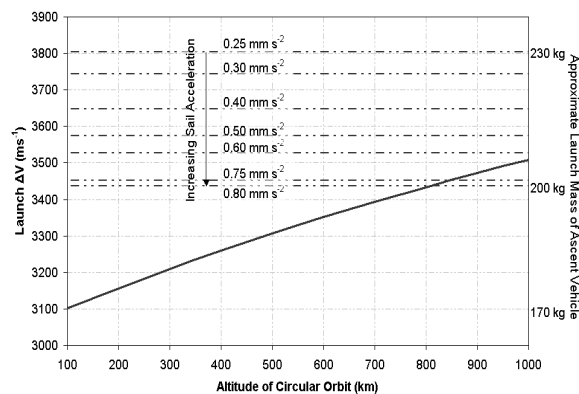


Figure 1: Mercury Ascent Vehicle rendezvous orbit trade-off (solid line: ascent to circular orbit, dashed lines: ascent to elliptical Sun-Synchronous orbit)

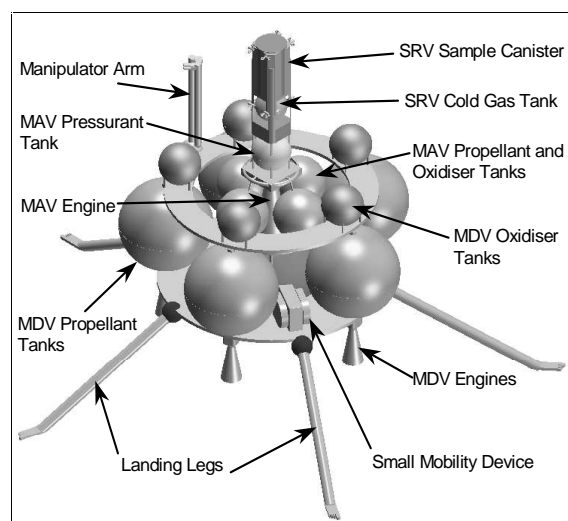


Figure 2: Mercury Sample Return lander

The SRV has a 2 kg sample container which holds the surface samples, with 50 m s^{-1} of propellant allocated for the rendezvous manoeuvre. The MAV uses a single stage DASA S3K class bi-propellant MMH/MON-3 engine, with a specific impulse of 352 s. However, volume reductions and an increase in thrust to 4 kN would be necessary. The MDV uses 5 bi-propellant MMH/MON-3 engines, delivering 6 kN each with a specific impulse of 320 s. The SCS allows for on-orbit power generation via 6.25 m^2 Gallium Arsenide solar arrays. The SCS telecommunications system comprises low and medium-gain X-band systems, a high-gain X/Ka band system, and a UHF link with the lander. The telecommunications systems have been sized to ensure adequate data return for the mission. A 28 volt, three domain, regulated power system is used. The SCS requires 332 W in Sunlight and 310 W during eclipse, met by 365 W 6.25 m^2 GaAs solar arrays, and 349 Wh Lithium-Ion batteries. The MDV requires 71 W, met through a 78 W 0.4 m^2 GaAs solar array. The 56 W MAV power requirement is attained through 53 Wh Li-Ion batteries. The SRV requires 24 W, provided by a 221 Wh Li-Ion battery over the SRV operational lifetime. The ballistic Earth Return Vehicle (ERV) uses a 41 Wh Primary Lithium battery to provide 1.7 W of power.

Science Instruments

The on-orbit SCS science payload includes a High Resolution Stereo Camera (10 W, 10-100 bps), Laser Altimeter (10 W, <1 bps), Infra-Red Radiometer (5 W, 100-5000 bps), X-ray Fluorescence Spectrometer (10 W, 100-2000 bps), Radio Science Instruments (5 W, 10-100 bps), and associated high-capacity memory (5 W, 2-5 Gbytes). There is also an 8 kg allocation for a payload of opportunity (10 W, 5 kbps).

The lander has science instruments and manipulator hardware mounted on the MDV, which include a Sampling Device, Robotic Arm, and a small Rover vehicle. The total data rate of these instruments corresponds to 92 Mbit every 10 hours, with a total power consumption of 11.8 W.

SRV Component	Mass (kg)	Contingency (%)	Total mass (kg)
Sample container	2.0	-	2.0
SRV Payload Mass	2.0	-	2.0
Attitude control	3.1	10	3.4
Command & data	0.5	10	0.6
Power	2.0	10	2.2
Mechanisms	0.1	10	0.1
Telecomms	1.1	10	1.2
Thermal	1.0	10	1.1
Structure	2.0	10	2.2
SRV Bus Mass	9.8	10	10.9
Thrusters	0.2	15	0.23
Valves, pipes	0.1	15	0.1
Propellant tank	0.1	15	0.1
Propulsion Mass (Dry)	0.4	15	0.43
SRV Dry Mass	12.2		13.3
System contingency	-	1	0.1
Total SRV Dry Mass			13.4
Propellant for rendezvous	1.0	15	1.1
Total SRV Mass (Wet)			14.5

Table 1: Sail Rendezvous Vehicle (SRV) system sheet mass breakdown

MAV Component	Mass (kg)	Contingency (%)	Total mass (kg)
SRV	14.5	-	14.5
MAV Payload Mass	14.5	-	14.5
Attitude control	4.5	10	4.9
Command & data	2.5	10	2.7
Power	2.3	10	2.5
Mechanisms	0.5	10	0.6
Telecomms	0.0	10	0.0
Thermal	2.0	10	2.2
Structure	5.2	10	5.7
MAV Bus Mass	17.0	10	18.6
Thruster	15.0	15	17.3
Valves, pipes	2.9	15	3.3
Propellant tank	9.5	15	10.9
Propulsion Mass (Dry)	27.4		31.5
MAV Dry Mass	58.9		64.6
System contingency	-	1	0.65
Total MAV Dry mass			65.3
Propellant for Δv_1	0.5	15	0.6
Propellant for Δv_2	94.8	15	109.0
Total Propellant Mass	95.29	15	109.6
Total MAV Mass (Wet)			174.9

Table 2: Mercury Ascent Vehicle (MAV) system sheet mass breakdown

MDV Component	Mass (kg)	Contingency (%)	Total mass (kg)
MAV	174.9	-	174.9
Surface instruments	2.9	-	2.9
MDV Payload Mass	177.8		177.8
Attitude control	15.0	10	16.5
Command & data	4.0	10	4.4
Power	8.8	10	9.7
Mechanisms	22.0	10	24.2
Telecomms	0.0	10	0.0
Thermal	3.0	10	3.3
Structure	83.0	10	91.3
MDV Bus Mass	135.8	10	149.4
Thrusters (5 of 6kN)	50.0	15	57.5
Valves, pipes	8.3	15	9.5
Propellant Tanks	83.0	15	95.5
Propulsion Mass (Dry)	141.3	15	162.5
MDV Dry Mass	454.9		489.7
System contingency	-	1	4.9
Total MDV Dry Mass			494.6
Propellant for Δv_1	4.0	15	4.6
Propellant for Δv_2	830.8	15	955.4
Total Propellant Mass	834.8	15	960.0
Total MDV Mass (Wet)			1454.6

Table 3: Mercury Descent Vehicle (MDV) system sheet mass breakdown

SCS Component	Mass (kg)	Contingency (%)	Total mass (kg)
Lander (SRV/MAV/MDV)	1454.6	-	1454.6
Science payload	31.6	-	31.6
ERV	16.5	5	17.3
SCS Payload Mass	1502.7		1503.5
Attitude control	14.1	10	15.5
Command & data	10.0	10	11.0
Power	40.2	10	44.2
Mechanisms	161.0	10	177.1
Telecomms	24.6	10	27.1
Thermal	50.0	10	55.0
Structure	65.4	10	71.9
SCS Bus Mass	365.3	10	401.8
Total Sail Payload Mass			1905.3

Table 4: Sail Cruise Stage (SCS) system sheet mass breakdown

SOLAR SAIL SIZING

A square solar sail is envisaged, using tip-vanes for attitude control, sized to provide adequate slew rates for the planet-centred mission phases. The spacecraft (sail payload) is mounted centrally, within the plane of the solar sail, so that both faces of the core structure are free to be used as attachment points for the lander, and Earth return capsule. Fig. 3 shows approximate trip times from Earth to Mercury, generated using methods described in the Trajectory Analysis section. An outbound trip time of 2-3 years is desirable to be competitive with SEP and Chemical Mercury trip times. This is enabled by a characteristic acceleration of 0.25 mm s^{-2} . The chosen sail conceptual design used in this paper is based on the AEC-ABLE Scaleable Solar Sail Subsystem (S^4), since it can be extrapolated to large sail dimensions.⁶ This design is based on Coilable booms, and the boom linear density as a function of length can be combined with NASA/LARC/SRS $2 \mu\text{m}$ or $5 \mu\text{m}$ CP1 film to obtain the sail assembly loading as a function of sail side length, shown in Fig. 4. It is assumed that conventional coatings are used, with Aluminium (85% reflectivity) on the frontside and Chromium (64% emissivity) on the backside. Fig. 4 also shows the necessary sail assembly loading as a function of sail side length, for delivery of a 1905 kg spacecraft to Mercury with a characteristic acceleration of 0.25 mm s^{-2} .

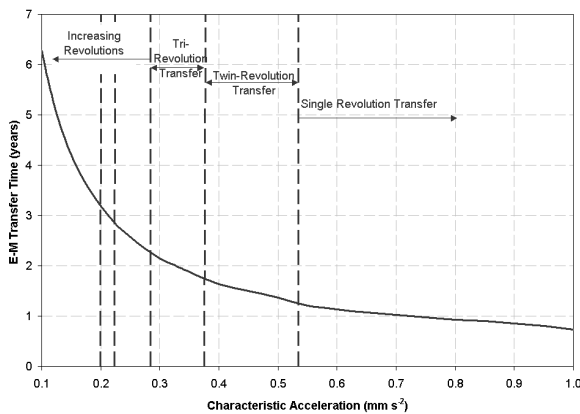


Figure 3: Approximate Earth-Mercury transfer time

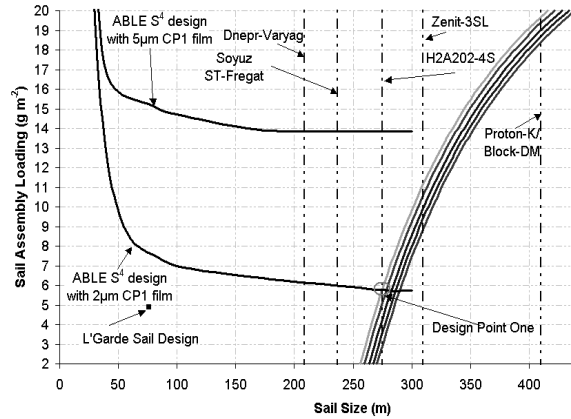


Figure 4: 0.25 mm s^{-2} solar sail design space (sail payload contours represent increasing parking orbit radius, with baseline 100 km orbit leftmost)

It can be seen that the intersection of the $2 \mu\text{m}$ CP1 ABL S^4 sail design curve with the 0.25 mm s^{-2} , 100 km orbit payload curve yields the sail design point, with an assembly loading of 5.9 g m^{-2} and sail dimensions of $275 \times 275 \text{ m}$. The design point and resultant characteristic accelerations during different points in the mission, as the lander is deployed and sample is returned, are shown in Table 5. It is important to stress that for a specific solar sail, the acceleration will increase as the solar sail payload mass is reduced, through the jettison of used modules.

Parameter	Value
Sail Assembly loading (@ 40% contingency)	5.9 g m^{-2}
Sail side length	275 m
Sail area (@ $2 \mu\text{m}$ thickness)	75625 m^2
Boom length	194 m
Sail reflective efficiency	0.85
Characteristic Acceleration (Earth departure)	0.25 mm s^{-2}
Characteristic Acceleration (Sample acquisition)	0.7367 mm s^{-2}
Characteristic Acceleration (Mercury departure)	0.7839 mm s^{-2}

Table 5: Solar sail specifications and resultant characteristic acceleration during each phase

A 275 m sail with an assembly loading of 5.9 g m^{-2} has a mass of 448 kg, with a mass budget as shown in Table 6. A linear boom density of 70 g m^{-1} is required with 0.94 m diameter to maintain a factor of safety against buckling. The total launch mass is therefore 2353 kg, which enables the use of an H2A202-4S class launch vehicle to escape velocity. The spacecraft stack with stowed sail is depicted within the H2A fairing in Fig. 5.

Component	Mass (kg)
Total payload mass	1905
2 μm CP1 film (@ 2.86 g m^{-2})	216
0.1 μm Al coating (@ 0.54 g m^{-2})	41
Bonding (@ 10% coated mass)	26
Sail booms (ABLE 0.94m booms @ 70 g m^{-1})	54
Mechanical systems (@ 40% contingency)	111
Total sail assembly mass	448
Total mission launch mass	2353
H2A202-4S capacity to $C_3 = 0$	2600
Launch mass margin	247 kg (9.5 %)

Table 6: Solar sail design point data set

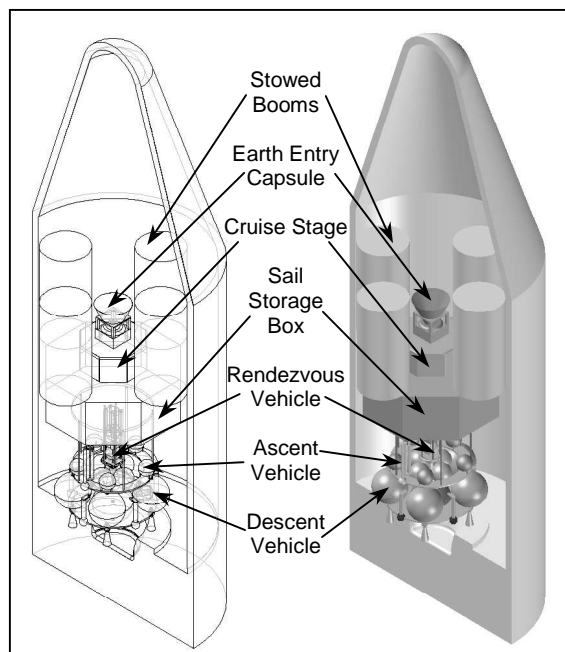


Figure 5: Payload stack in H2A 202-4S fairing

COST ANALYSIS

The spacecraft has been costed using parametric Cost Estimating Relationships (CERs).⁷ Conservative margins have been added, and the cost of specialist components, such as bi-propellant engines, have been taken from NASA/JPL Team X estimates.² Project management and integration and support costs are also estimated using Ref. 7. The most difficult system to cost is that of the solar sail, since a sail is yet to fly, let alone one of 275 m dimension. A crude estimate leads to a ROM cost of 28.4 M€, but it should be noted the cost of the sail is small in comparison with the spacecraft itself. In addition, the reduction in launch cost compared with conventional concepts more than makes up for sail cost.

Conservative cost margins of 30% have been added to give the mission cost breakdown shown in Table 7. The total solar sail Mercury sample return mission ROM cost is therefore of order 850 M€. We note that, although the launch cost is fairly low, the predominant cost component is the spacecraft itself, which is mostly independent of the primary propulsion method used. Traditionally, solar sailing is seen to be superior to chemical propulsion or SEP, if it can reduce launch mass and cost, but for a sample return mission, the sail must *significantly* reduce launch mass, for there to be any appreciable reduction in overall mission cost.

Component	Cost (FY03M€)	Margin (%)	Total Cost (FY03M€)
SRV	27.8	30	36.1
MAV	58.8	30	76.4
MDV	88.3	30	114.8
SCS	89.1	30	115.8
SOLAR SAIL	28.4	30	36.9
EEV	4.2	30	5.5
Spacecraft Cost	296.6	-	385.5
IA&T	94.9	30	123.4
Program Level	156.3	30	203.2
GSE	19.6	30	25.5
LOOS	18.1	30	23.5
Launch Cost (H2A)	83.9	10	92.3
Associated Costs	372.8	-	467.9
Total Mission Costs	669.4	-	853.4

Table 7: Cost breakdown

TRAJECTORY ANALYSIS

The required Δv for direct ballistic transfer to a low Mercury parking orbit is of order 13 km s^{-1} . Chemical propulsion and Solar Electric Propulsion (SEP) both require a prolonged sequence of gravity assists to reduce launch mass. Mercury sample return from deep within the solar gravity well is one of the most energetically demanding mission concepts imaginable. However, propellant mass is not an issue here and the sail can spiral directly to the planet, making best use of the inverse square increase in Solar Radiation Pressure (SRP) at lower heliocentric radii. Many authors have recognised the benefit of solar sailing to reach Mercury, but this paper provides new data sets by considering both launch windows, and return trajectories.

Heliocentric trajectories have been optimised using the constrained parameter optimisation algorithm, NPSOL, based on Sequential Quadratic Programming (SQP).^{8,9} Engineering insight coupled with 'incremental feedback' methods were used to obtain initial guesses for optimisation. Planet centred manoeuvres are modelled using a set of blended analytical control laws.¹⁰ Mercury capture and escape trajectories have been generated mainly using a control law which maximises the rate of change of orbit energy. Many control laws are blended for Mercury-centred transfer manoeuvres.

Launch windows

Fig. 6 shows the Earth departure date scan for the selected characteristic acceleration of 0.25 mm s^{-2} , over a 3 year period. Each point on the curve represents an optimisation at that launch date. It is seen that the minimum time launch opportunities occur once every year. Solar sailing is not restricted to launch windows, but it is clear that a saving of 300 days can be achieved depending on launch date. The discontinuities posed problems when incrementing the launch date to find initial guesses for other launch dates. These discontinuities are due to the spacecraft 'just missing' the target and having to execute another revolution of the Sun to reach Mercury. To determine the optimal launch date, consideration must also be given to the

variation of the capture and escape times along Mercury's orbit, and the return Mercury-Earth phase. Since Mercury has an eccentricity of 0.2056, then the available SRP will vary over a Mercury year.¹¹ Approximate capture and escape times are shown in Fig. 7, for the accelerations specified in Table 5.

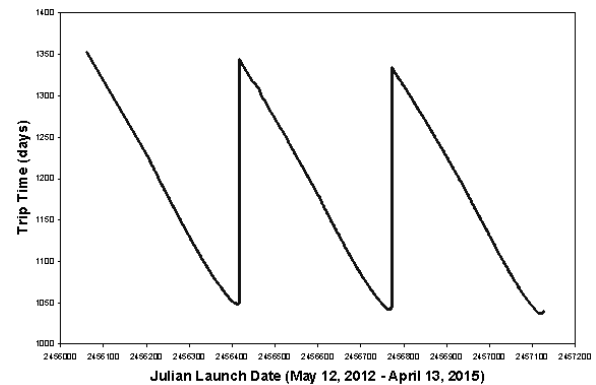


Figure 6: Earth-Mercury departure date scan

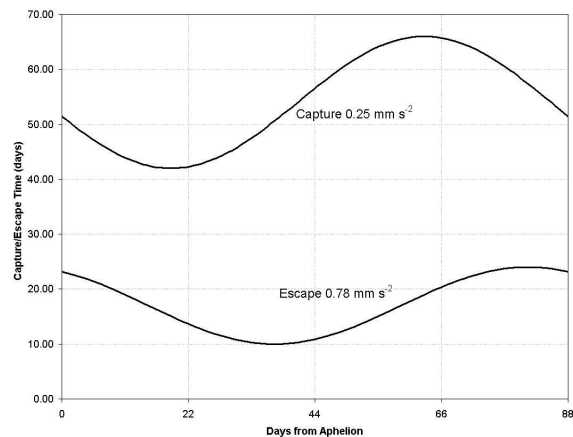


Figure 7: Mercury capture/escape time variation

With an orbiter stay time of order 40 days, Figs. 6 and 7 can be used to ascertain that the return scan was only required across a 2 year range (small variation). The 4 curves were then mapped together to determine the overall mission duration as a function of Earth departure date. This is shown in Fig. 8, where it is clear that the long duration outbound spiral dominates the total mission duration. The launch opportunity selected was that on April 19, 2014.

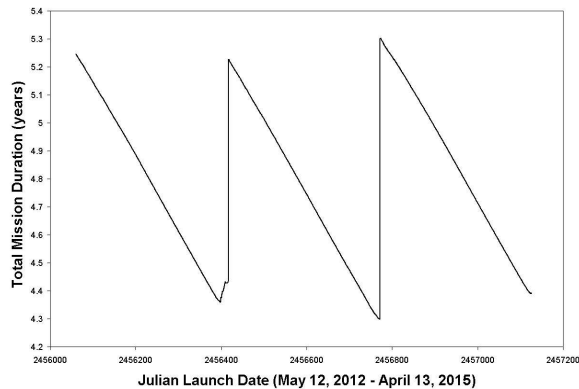


Figure 8: Total mission duration launch opportunities

Earth-Mercury Phase

The outbound trajectory is shown in Fig. 9, departing Earth with C_3 of zero on April 19, 2014. Mercury arrival is on February 24, 2017, 2.85 years later, after $5 \frac{1}{4}$ revolutions. The optimal cone and clock control angles are shown in Fig. 10. Even at a relatively coarse control resolution of 50 linear interpolation segments, the profiles are smooth and oscillatory.

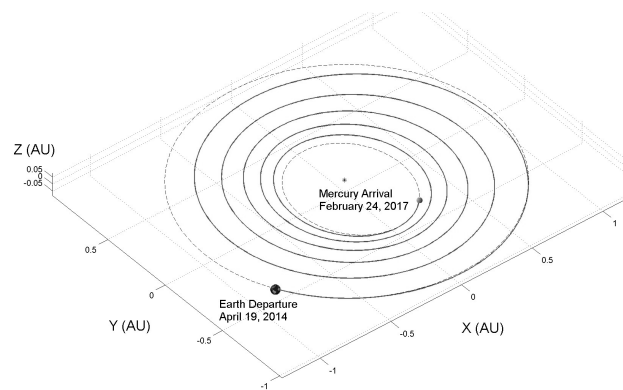


Figure 9: Earth-Mercury trajectory

The reduction in heliocentric radius and subsequent increase in sail film temperature is depicted in Fig. 11. Equilibrium sail film temperature is modelled using a black body approximation, assuming temperature changes take place instantaneously, since the micron-scale thickness of the film ensures that the thermal inertia is effectively zero. Aluminium/Chromium coatings are assumed

as was discussed previously. The temperature is a function of both the radius and the sail attitude, with a maximum value of 443.7 K. Even face on to the Sun at Mercury perihelion, the worst-case temperature would be 494.5 K, still less than the predicted 520 K upper limit of polyimide films.

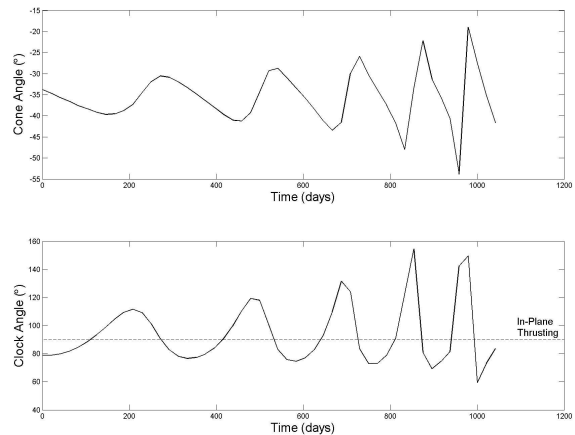


Figure 10: Earth-Mercury control angle profile

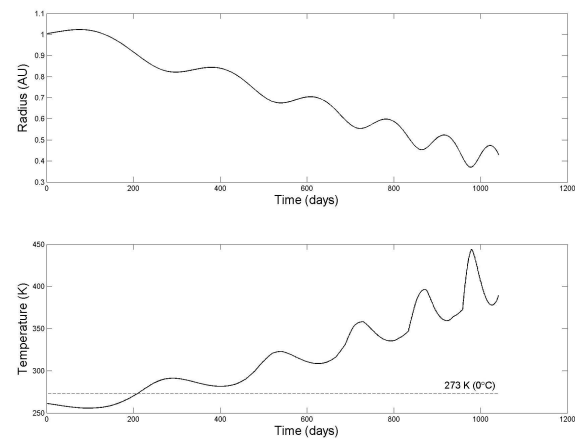


Figure 11: Earth-Mercury heliocentric radius and sail film temperature

Mercury Centred Manoeuvres

It has been assumed that the sail arrives at Mercury with zero hyperbolic excess velocity. The transition from heliocentric to planet-centred motion has not been patched. However, it is assumed that the sail can be used to correct for approach dispersion and can target the correct B-plane for capture. As

has been prescribed, capture is into a 100 km x 7500 km Sun-Synchronous polar orbit, 10° ahead of the terminator, before subsequent manoeuvring into the 100 km parking orbit. This capture spiral takes 28 days and is shown in Fig. 12, arriving on orbit on March 24, 2017.

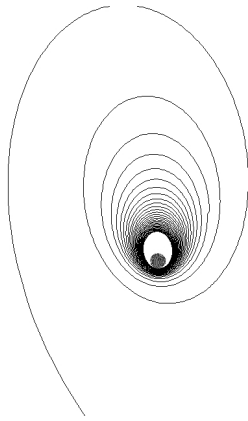


Figure 12: Mercury capture spiral into 100 km x 7500 km Sun-Synchronous polar orbit

131 days will be available for orbital science operations, surface observation and final manoeuvring to the lander descent orbit. This orbiter stay-time is also a requirement due to the thermal environment on the surface. The thermally-benign, Sun-Synchronous orbit (10° ahead of terminator) is forced for 44 days until the orbit is in the correct orientation for the landing site. The sail then waits in this orbit for 37 days. Next, a 50 day manoeuvre transfers the spacecraft to the 100 km polar orbit, where the lander begins its descent on August 3, 2017. Once on the surface, the lander carries out 4 days of sample acquisition and landing site documentation operations. The solar sail is used to rotate the orbit plane to account for Mercury landing site rotation, so that the MAV ascends in a coplanar manoeuvre. The orbit plane cannot be rotated as fast as Mercury spins, so the MAV will need to wait in the 100 km orbit (thermally-safe) until solar sail rendezvous with the MAV. Final proximity manoeuvring is accomplished with the SRV, thereby relaxing MAV launch accuracy. Rotation of the orbit plane to match that of the landing site is depicted in Fig. 13. After sample transfer to the Earth Return Vehicle attached to the sail, the solar sail spirals to

escape. A method which maximises the rate of change of orbit energy while maintaining a positive altitude of periapsis is illustrated in Fig. 14. The escape spiral is initiated on August 18, 2017, with escape reached in 16 days.

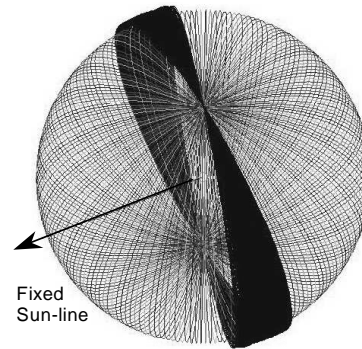


Figure 13: Rotation of 100 km polar orbit plane to match coplanar MAV ascent trajectory

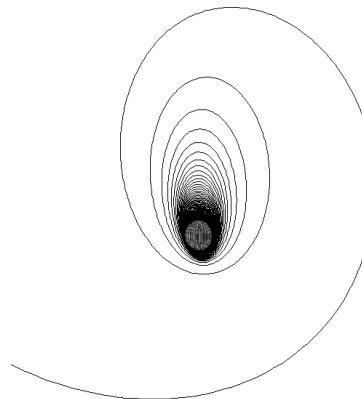


Figure 14: Mercury escape spiral from 100 km circular polar orbit

Mercury-Earth Phase

Return heliocentric spiralling commences after Mercury escape on September 3, 2017. The trip time is 369 days, with arrival back at the Earth with zero hyperbolic excess on September 8, 2018. Fig. 15 shows the 2 revolution trajectory, which is faster because the sail characteristic acceleration has increased to 0.78 mm s^{-2} . The cone and clock angle control profile is shown in Fig. 16. Finally, the ERV spins up and is separated to perform a ballistic entry for sample delivery to Earth. The total mission duration is 4.39 years.

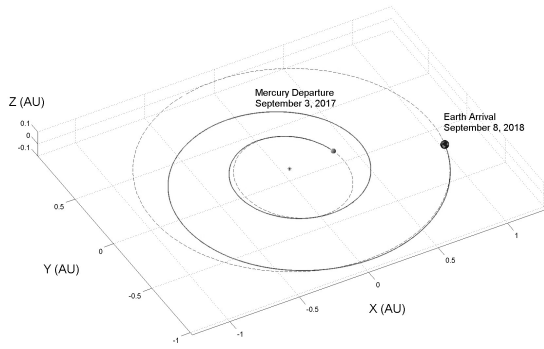


Figure 15: Mercury-Earth trajectory

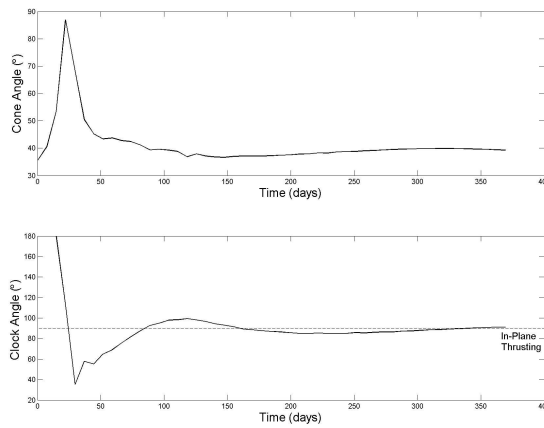


Figure 16: Mercury-Earth control angle profile

Alternative trajectory Options

Use of a positive launch C_3 against the Earth's velocity would be highly advantageous for reaching close solar orbits such as that of Mercury. The initial eccentricity for the inward spiral can be easily circularised by the increased solar radiation pressure closer to the Sun. Fig. 17, shows the effect of using excess launch energy to reduce the trip time to Mercury orbit. It can be seen that the effect is greater for lower accelerations, since the trip time is longer and there are more revolutions for $C_3=0$. The use of a Zenit 3-SL over an H2A, would allow for a $C_3 = 8 \text{ km}^2 \text{ s}^{-2}$, which would reduce the outbound trip time by 260 days, for the same launcher cost.

Fig. 18 shows that the inclusion of a Venus gravity assist could reduce the outbound trip time by 140 days (see Ref. 8), but gravity

assists are not essential for solar sails since propellant mass is not an issue.

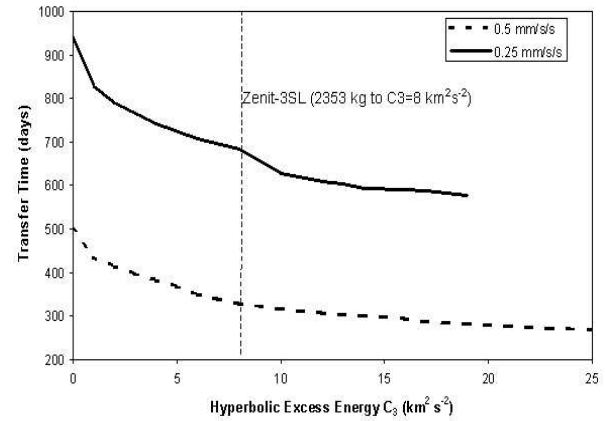


Figure 17: Effect of hyperbolic excess energy at launch

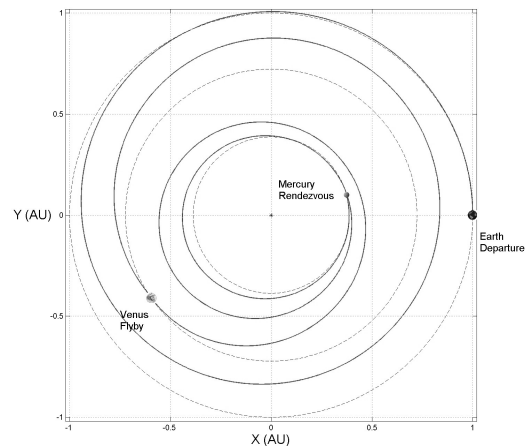


Figure 18: Venus gravity assist

MISSION EVALUATION AND CONCLUSION

Other possible mission architectures were considered in the course of this work.⁴ In addition to the baseline all-sail concept, the use of the sail to spiral to Earth escape to reduce launch energy requirements was considered, a multi-mission concept, and a chemical/sail hybrid mission was briefly investigated. A chemical outbound ballistic transfer to Venus, with a small solar sail deployed for return, is attractive.¹² However, the outbound gravity assisted trajectory to Mercury would dominate the mission duration

of almost 9 years, even though a smaller, cheaper solar sail could be used for the return leg. An Ariane 5 launch would be required in this case.

To summarise the Solar Sail MeSR concept, a 275 m side square solar sail is used to transport a 1905 kg payload to 100 km polar orbit at Mercury, and return a sample to Earth in 4.4 years. The 448 kg, 5.9 g m^{-2} solar sail uses AEC-ABLE booms and $2 \mu\text{m}$ CP1 film, with conventional coatings. The launch mass of 2353 kg is lifted using an H2A202-4S ($C_3=0$, or Zenit-3 SL to $C_3=8$). The total mission ROM cost is estimated to be 850 M€.

The mission concept has been compared with other propulsion options.^{1,2} The 5775 kg launch mass of the NASA/JPL Team X SEP concept requires an Atlas V 551 launcher, for a 6.9 year mission, costing of order 1034 M€.² An ESA Chemical/SEP concept has a 6500 kg launch mass on an Ariane 5E, for a mission duration of 7.2 years.¹ No ROM cost is given for this, but it is expected to be in the same order of the NASA cost. Therefore, it is clear that a solar sail MeSR mission can reduce the total mission duration by 40%, and reduce launch mass by 60%, with a reduction in ROM cost of at least 180 M€.

Finally, this analysis assumes the feasibility of large sail structures, their deployment, and attitude control using tip-vanes. There is limited experience of large gossamer structures at present. Therefore, it is imperative that near-term demonstration missions take place, and a rigorous technology development programme is pursued, before a solar sail mission to Mercury can be realised.

ACKNOWLEDGEMENT

This work was performed under ESA/ESTEC contract 16534/02/NL/NR – Technical Assistance in the Study of Science Payloads Transported through Solar Sailing.

REFERENCES

1. Scoon, G., Lebreton, J-P., Coradini, M., et al, "Mercury Sample Return", Assessment Study Report, ESA Publication SCI(99)1, 1999.
2. Oberto, B., et al, "Mercury Sample Return 2002-01," Team X Advanced Projects Design

Team Report, Jet Propulsion Laboratory, Pasadena, California, 2002.

3. McInnes, C. R., *Solar Sailing: Technology, Dynamics and Mission Applications*, Springer-Praxis Series in Space Science and Technology, Springer-Verlag, Berlin, 1999.
4. McInnes, C. R., Hughes, G. W., and Macdonald, M., "Technical Note 3 – Mercury Sample Return," ESTEC 16534/02/NL/NR, ESA/ESTEC Contract Report, University of Glasgow, 2003.
5. Leipold, M.E., Wagner, O., "Mercury Sun-Synchronous Polar Orbits Using Solar Sail Propulsion", J. Guidance, Control and Dynamics, Vol. 19, No. 6, pp 1337-1341, 1996.
6. Murphy, D.M., and Murphey, T.W., "Scalable Solar Sail Subsystem Design Considerations," AIAA 2002-1703, 43rd Structures, Structural Dynamics and Materials Conference, Denver, Colorado, Apr. 22-25, 2002.
7. Wertz, J. R., and Larson, W. J., *Space Mission Analysis and Design*, Kluwer Academic Publishers, pp 795-802, ISBN 0-7923-5901-1, 1999.
8. Hughes, G. W., and McInnes, C. R., "Mercury Sample Return Missions Using Solar Sail Propulsion," IAC-02-W-2.08, 53rd International Astronautical Congress, Houston, Texas, Oct. 10-19, 2002.
9. Hughes, G. W., and McInnes, C. R., "Small-Body Encounters Using Solar Sail Propulsion," *Journal of Spacecraft and Rockets*, Vol. 41, No.1, pp. 140-150, Jan.-Feb., 2004.
10. Macdonald M., and McInnes C. R., "Analytic Control Laws for Near-Optimal Geocentric Solar Sail Transfers," AAS 01-472, Advances in the Astronautical Sciences, Vol. 109, No. 3, pp. 2393-2413, 2001.
11. Macdonald M., and McInnes, C. R., "Seasonal Efficiencies of Solar Sailing in Planetary Orbit," IAC-02-S.6.01, 53rd International Astronautical Congress, Houston, Texas, Oct. 10-19, 2002.
12. Hughes, G. W., Macdonald, M., McInnes, C. R., Atzei, A., and Falkner, P., "Terrestrial Planet Sample Return Missions Using Solar Sail Propulsion," 5th IAA International Conference on Low-Cost Planetary Missions, ESA/ESTEC, The Netherlands, Sept. 24-26, 2003.